Mineralogical Magazine (2022), **86**, 688–700
doi:10.1180/mgm.2022.22

CAMBRIDGE UNIVERSITY PRESS

Article

Special Issue dedicated to Peter Williams

Linking derived debitage to the Stonehenge Altar Stone using portable X-ray fluorescence analysis

Richard E. Bevins[1,2]*, Nick J.G. Pearce[2,3], Rob A. Ixer[4], Stephen Hillier[5,6], Duncan Pirrie[7] and Peter Turner[8]

[1]Department of Natural Sciences, National Museum of Wales, Cathays Park, Cardiff CF10 3NP, UK; [2]Department of Geography and Earth Sciences, Aberystwyth University, Aberystwyth SY23 3DB, UK; [3]Dipartimento di Scienze Biologiche, Geologiche e Ambientali, Università di Bologna, 40126 Bologna, Italy; [4]Institute of Archaeology, University College London, London WC1H 0PY, UK; [5]The James Hutton Institute, Craigiebuckler, Aberdeen AB15 8QH, UK; [6]Department of Soil and Environment, Swedish University of Agricultural Sciences (SLU), SE-75007 Uppsala, Sweden; [7]School of Applied Sciences, University of South Wales, Pontypridd CF37 4BD, UK; and [8]7 Carlton Croft, Streetly, West Midlands B74 3JT, UK

Abstract

The Altar Stone at Stonehenge in Wiltshire, UK, is enigmatic in that it differs markedly from the other bluestones. It is a grey–green, micaceous sandstone and has been considered to be derived from the Old Red Sandstone sequences of South Wales. Previous studies, however, have been based on presumed derived fragments (debitage) that have been identified visually as coming from the Altar Stone. Portable X-ray fluorescence (pXRF) analyses were conducted on these fragments (*ex situ*) as well as on the Altar Stone (*in situ*). Light elements (Z<37) in the Altar Stone analyses, performed after a night of heavy rain, were affected by surface and pore water that attenuate low energy X-rays, however the dry analyses of debitage fragments produced data for a full suite of elements. High Z elements, including Zr, Nb, Sr, Pb, Th and U, all occupy the same compositional space in the Altar Stone and debitage fragments, and are statistically indistinguishable, indicating the fragments are derived from the Altar Stone. Barium compares very closely between the debitage and Altar Stone, with differences being related to variable baryte distribution in the Altar Stone, limited accessibility of its surface for analysis, and probably to surface weathering.

A notable feature of the Altar Stone sandstone is the presence of baryte (up to 0.8 modal%), manifest as relatively high Ba in both the debitage and the Altar Stone. These high Ba contents are in marked contrast with those in a small set of Old Red Sandstone field samples, analysed alongside the Altar Stone and debitage fragments, raising the possibility that the Altar Stone may not have been sourced from the Old Red Sandstone sequences of Wales. This high Ba 'fingerprint', related to the presence of baryte, may provide a rapid test using pXRF in the search for the source of the Stonehenge Altar Stone.

Keywords: Stonehenge, Altar Stone, sandstone, debitage, portable XRF, provenancing

(Received 20 September 2021; accepted 28 February 2022; Accepted Manuscript published online: 22 March 2022; Associate Editor: Eimear Deady)

Introduction

Stonehenge is one of the most iconic ancient historic monuments in Europe, first constructed in late Neolithic times, around 3000 B.C., though added to and reconfigured over the following 1500 years (Darvill *et al.*, 2012). Understanding the provenance of the megaliths used in the construction of the monument informs our understanding of early Neolithic populations, their distribution, and their interactions. Stonehenge is particularly important in this context in view of the long-distance transport of some of its stones, known as the 'bluestones'. These form the Bluestone Circle and the Bluestone Horseshoe and are considered to have been the first stones erected at Stonehenge, originally forming a single circle of 80 stones in the so-called Aubrey Holes around 3000 BC (see Parker Pearson *et al.*, 2020). They contrast with the much larger sarsen stones that form the Outer Sarsen Circle and the Inner Sarsen Trilithon Horseshoe.

The first major investigation of the provenance of the bluestones was undertaken almost 100 years ago by the eminent British geologist H.H. Thomas who was a surveyor and then petrographer with the (then) Geological Survey of Great Britain. Although there had been earlier studies, such as those by Maskelyne (1878), Teall (1894) and Judd (1902), Thomas's investigation was more detailed than the earlier works. In a seminal paper (Thomas, 1923) he concluded that the bluestones comprised dolerites, rhyolites and tuffs of Lower Palaeozoic age and that the majority could be sourced to a small area in the Mynydd Preseli, in north Pembrokeshire, west Wales, ~225 km to the west of Stonehenge (see Fig. 1).

One bluestone appeared anomalous, however. This stone, stone 80 (see Nash *et al.*, 2020, Fig. 1), also known as the Altar

***Author for correspondence:** Richard Bevins, Email: richard.bevins@honorary.museum-wales.ac.uk

This paper is part of a thematic set that honours the contributions of Peter Williams
Cite this article: Bevins R.E., Pearce N.J.G., Ixer R.A., Hillier S., Pirrie D. and Turner P. (2022) Linking derived debitage to the Stonehenge Altar Stone using portable X-ray fluorescence analysis. *Mineralogical Magazine* **86**, 688–700. https://doi.org/10.1180/mgm.2022.22

© The Author(s), 2022. Published by Cambridge University Press on behalf of The Mineralogical Society of Great Britain and Ireland. This is an Open Access article, distributed under the terms of the Creative Commons Attribution licence (http://creativecommons.org/licenses/by/4.0/), which permits unrestricted re-use, distribution and reproduction, provided the original article is properly cited.

https://doi.org/10.1180/mgm.2022.22 Published online by Cambridge University Press

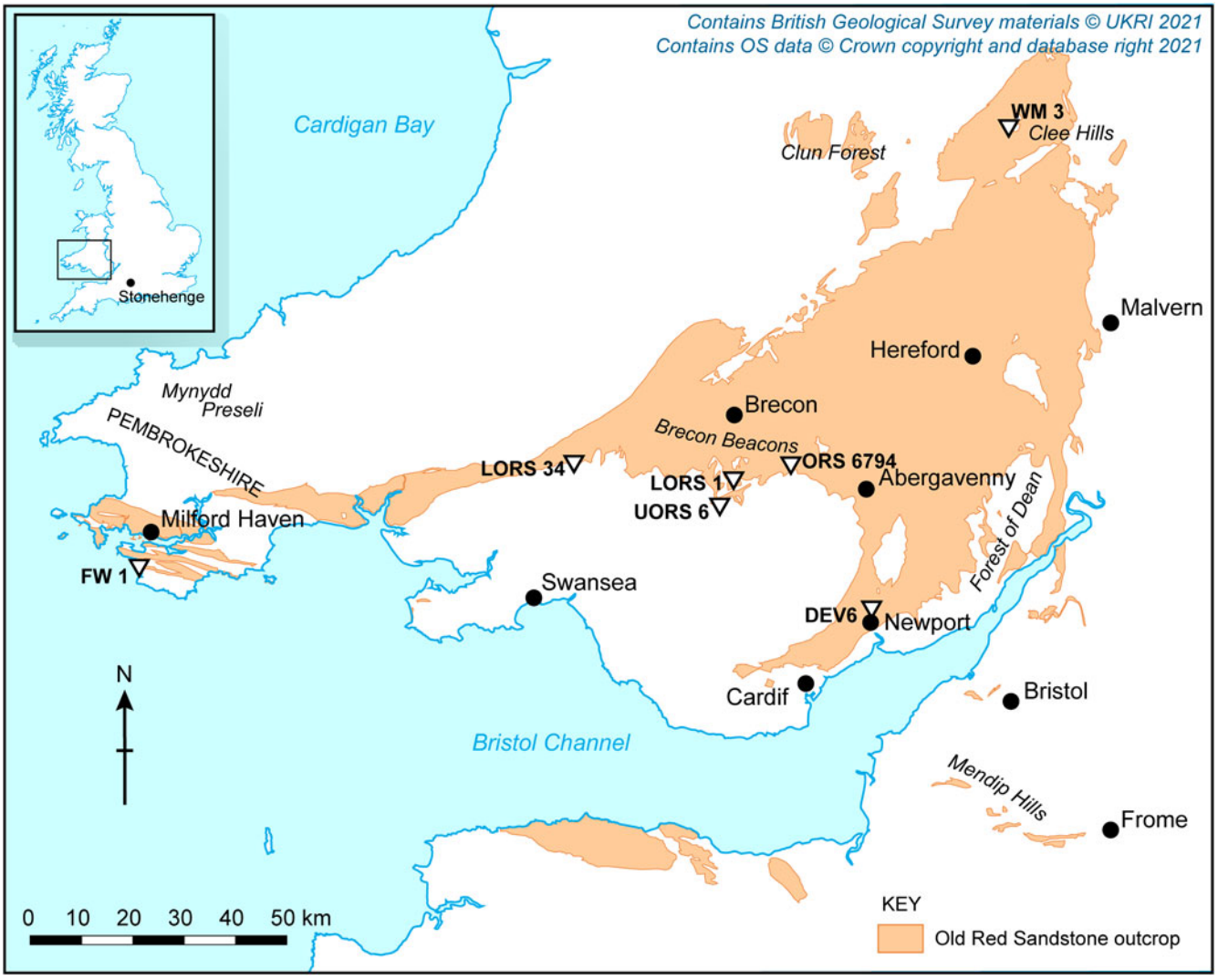

Fig. 1. Map showing the location of the Mynydd Preseli as well as the distribution of the Old Red Sandstone in southern Wales, the Welsh Borderland and southwest England, based on British Geological Survey Geology 625kDiGMapGB-625, together with sampling sites for the seven Old Red Sandstone samples analysed.

Stone, is a grey–green, micaceous sandstone of a type not found in the Mynydd Preseli area and Thomas (1923) considered that it might be from either the Cosheston Group (now called the Cosheston Subgroup) or the Senni Beds (now called the Senni Formation), both part of the Old Red Sandstone Supergroup (of late Silurian to Devonian age), exposed elsewhere in South Wales. The Altar Stone is the largest of the bluestones, measuring 4.9 m long by 1 m wide by 0.5 m thick as seen in the archive photographs in Fig. 2c,e dating from 1958, although it is currently less well exposed (see Fig. 2a–b, f). It is estimated to weigh six tonnes. It is partly covered by two fallen sarsen (trilithon) stones, one of which (stone 55b) appears to have broken the Altar Stone (Fig. 2c). In view of the current exposure, we have labelled the three currently exposed areas of the Altar Stone as areas A, B and C (Fig. 2a,b and f).

Realising that standard transmitted and reflected light microscopy had essentially reached the limits of their application to advance our understanding of the character and provenance of the bluestones we have, over the last 10 years, employed a range of advanced analytical techniques in our investigations. Thorpe *et al.* (1991) and Bevins *et al.* (2012, 2014) used whole-rock standard X-ray fluorescence spectrometry to some effect in provenancing some of the bluestone dolerites and one type of rhyolite. More recently we have used U–Pb zircon age determination, inductively coupled plasma-mass spectrometry, and automated scanning electron microscopy with energy dispersive spectroscopy (SEM-EDS) in our investigations of the bluestones, for example as in Bevins *et al.* (2020) for the Altar Stone, and Bevins *et al.* (2021) for further refinement of the provenance of the Group 2 dolerites of Bevins *et al.* (2014).

To date, all investigations of the Altar Stone have been based entirely on presumed derived fragments ('debitage') linked solely on macroscopic (hand specimen) and more lately microscopic similarities. There is no evidence for direct sampling of the Altar Stone in historic times. In this context, it is imperative to ascertain if the presumed Altar Stone fragments are indeed derived from the Altar Stone so that analytical data from investigations on the fragments can be used with confidence in our search for the original source of the Altar Stone.

Recent studies

The first detailed investigation of the Altar Stone was the petrographic study by Ixer and Turner (2006) of historic thin section Wiltshire 61 277 (from the South-Western Group of Museums

https://doi.org/10.1180/mgm.2022.22 Published online by Cambridge University Press

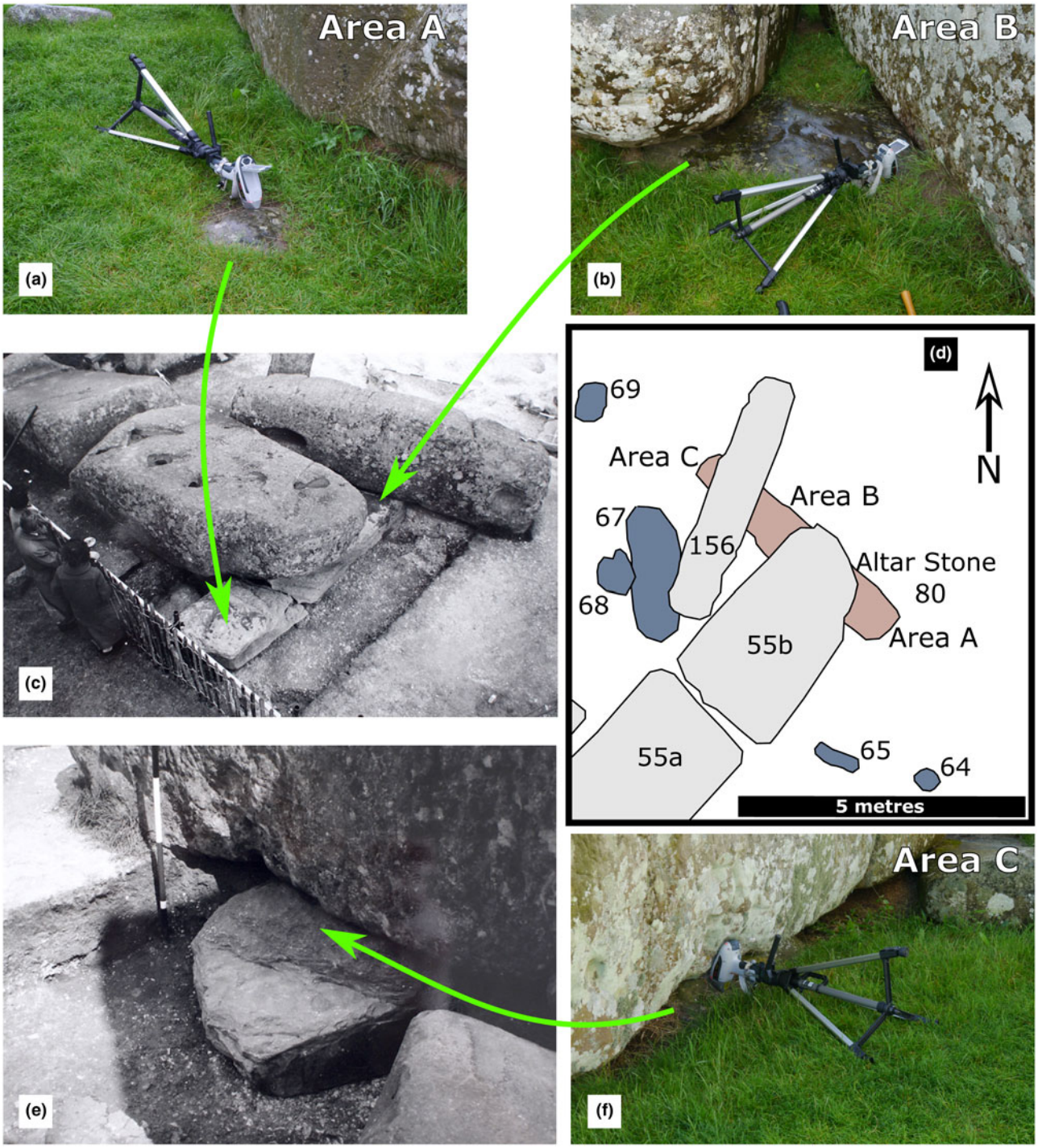

Fig. 2. Locations of areas of the Altar Stone (stone 80) at Stonehenge analysed by portable XRF. (a) Area A at the eastern end of the Altar Stone to the left of the fallen upright of the Great Trilithon (stone 55b); (b) Area B, the central part of the Altar Stone between stone 55b and the lintel of the Great Trilithon (stone 156); (c) historic photograph of Areas A and B lying beneath stone 55b and apparently broken by it; (d) map showing disposition of the analysed areas on the Altar Stone (brown) and other near-by stones including bluestones (bluestones 64–69) and parts of the Great Trilithon and its lintel (grey, stones 55a, 55b and 156); (e) historic photograph of Altar Stone Area C lying beneath stone 156; (f) the western edge of the Altar Stone (Area C), under the lintel of the Great Trilithon (stone 156). Note standing water on the surfaces of the stones. For scale the metal part of the leg of the tripod is 41 cm long. Fig 2c,e reproduced with permission of Historic England.

and Art Galleries Implement Petrology Collection held at the Somerset Heritage Centre, Taunton, UK). Based on the assumption that this sample was derived from the Altar Stone they concluded that the Altar Stone was not derived from the Cosheston Subgroup, but that it is petrographically very similar to sandstones from the Senni Formation.

Ixer *et al.* (2019) reviewed all known presumed Altar Stone fragments held in museum collections and noted the general uniformity of their petrography. They dismissed two thin sections claimed to be 'Altar Stone' held by the Hunterian Museum as not being derived from the Altar Stone, as one is a volcanic tuff and the other a sandstone with little carbonate. They proposed

https://doi.org/10.1180/mgm.2022.22 Published online by Cambridge University Press

that sample SH08 Context 1 FN196 (from the 2008 excavation at Stonehenge by Darvill and Wainwright and hereafter referred to as FN196) would be a better 'type specimen', noting that Wiltshire 61 277 may well be atypical. Ixer *et al.* (2020) presented new preliminary mineralogical evidence that showed the presumed Altar Stone fragments were not sourced from the Cosheston Subgroup sequences exposed in the vicinity of Milford Haven, in west Wales (Fig. 1), instead proposing a more likely source in eastern Wales or the Welsh Borderland.

Bevins *et al.* (2020) elaborated on Ixer *et al.* (2020), presenting detailed analytical data of six presumed Altar Stone fragments using automated SEM-EDS to show that the fragments all have very similar modal mineralogy and that there is a strong likelihood that they were all derived from a single block of sandstone. They compared the modal mineralogy of these six fragments with those of three Lower Palaeozoic Sandstone fragments from Stonehenge (see Ixer *et al.*, 2017) and three samples from the Cosheston Subgroup in west Wales. The data presented by Bevins *et al.* (2020) clearly showed that the Lower Palaeozoic Sandstone and the Cosheston Subgroup sandstones were different from each other, and both were different to the presumed Altar Stone fragments. A key observation of this study was the presence of significant modal proportions of baryte in the presumed Altar Stone fragments (modal proportions in the range 0.29–0.80%), a mineral not seen in the Lower Palaeozoic Sandstone and as only a trace (0.01%) in two of the three Cosheston Subgroup samples. Bevins *et al.* (2020) also undertook radiometric age determinations of zircons in one of the presumed Altar Stone fragments and in a Cosheston Subgroup sample. They showed that the Cosheston Subgroup zircon age population was essentially bimodal, with maxima at 500 and 1500 Ma, whilst the presumed Altar Stone fragment zircon population was more diverse, with ages spanning 472 to 2475 Ma and showing no maxima. This again served to demonstrate that the presumed Altar Stone fragments were not derived from the Cosheston Subgroup in west Wales.

In this paper we focus on the six presumed Altar Stone fragments and compare their composition with the Altar Stone itself based on portable X-ray fluorescence (pXRF) analysis. The purpose of this study is to determine if we can match the fragments to the Altar Stone in order to use the fragments as a proxy for the Altar Stone itself. If this is the case then mineralogical and geochemical data obtained to date from the fragments can be used to 'fingerprint' the Altar Stone, aiding our search for its provenance without requiring sampling, compromising the integrity of the Altar Stone itself. We also intend to determine whether rapid pXRF analysis of sandstone field samples might provide a viable means of testing for a potential source for the Altar Stone by comparing analyses of a small set of Old Red Sandstone samples from Wales and the Welsh Borderland.

Samples studied and methods

Samples studied

Samples analysed in this investigation are shown in Table 1 which explains their lithological grouping and relevant contextual details together with reference to any previous petrographical descriptions. In addition to the *in situ* Altar Stone, which was analysed in July 2021, the samples investigated comprised: three probable Altar Stone fragments from excavations at Stonehenge in 2008 (Darvill and Wainwright, 2009); three probable Altar Stone fragments from an excavation near stone 1 by Colonel Hawley in 1920; six field samples of Old Red Sandstone (ORS) collected from across South Wales and the Welsh Borderland (Hillier *et al.*, 2006) and one unpublished field sample from the Old Red Sandstone near Llangynidr, Powys, Wales. The distribution of the samples from the ORS is shown in Fig. 1.

Portable X-ray fluorescence and some of its limitations

Portable X-ray fluorescence analyses (pXRF) were performed using a Thermo Fisher Scientific™ Niton™ XL3t GOLDD+ handheld XRF analyser. The Niton pXRF uses a 2 W Ag anode X-ray tube, which can operate at between 6–50 kV and 0–200 μA, with operating conditions being varied during the 'TestAllGeo' analysis method. This allows determination of a range of elements in geological materials from Mg to U by use of different filters that operate in sequence together to optimise sensitivity. The elements determined nominally in each mode are given in Table 2, during a total analysis time of 100 s. An 8 mm diameter analysis spot was used for all analyses, and the spectra were collected on a silicon drift detector, processed and calibrated by the manufacturer-installed instrument calibration. To ensure day-to-day consistency of the pXRF analyses, a sample of obsidian from the Big Obsidian Flow (BOF) at Newberry Volcano, Oregon, USA, was analysed repeatedly to monitor the calibration. The results from different analytical sessions did not change significantly during the analyses for this study, meaning data from different sessions can be compared. Data for the analyses of the Newberry BOF are listed in Supplemental Table S1, and show that the day-to-day precision is good for elements including Rb, Zr, Sr, Nb, K, Ca, Al, Si and Fe (∼±3–4%), slightly worse for Ba and Mn (∼8%), and lower again for Th and U (∼8–13%), however all are within the range of all analyses of the BOF performed over the last year as part of our provenance investigations. These levels of day-to-day precision allow confident comparisons to be made between pXRF analyses. Some published averages for multiple bulk sample analyses of the Newberry BOF (Laidley and McKay, 1971; Higgins, 1973; Linneman, 1990) by XRF, atomic absorption spectroscopy, gamma and other spectroscopic analyses, are also presented in Supplemental Table S1. These show that the pXRF results here (from a sample of the flow near the flow front, but not directly related to the samples analysed in the various publications) are in broad agreement (<±15%) for many elements (Rb, Ba, Zr, Fe, Mn, Al, Si, K, Ti and Th), suggesting an acceptable level of accuracy for the current pXRF analyses. Somewhat worse (∼ ±25–30%) are Sr and Ca, though these variations may relate to the specific BOF sample analysed here. However, unrealistically high concentrations were recorded for Cd and Sc by pXRF (78,000 ppm and 10,000 ppm respectively). This attests to some calibration/spectral recognition issues within the Niton instrument which, when analyses are performed using all filter modes, appear to mis-identify the Compton-scattered source radiation peak as extreme concentrations of these elements.

Limits of detection (LoD) in pXRF, calculated by the instrument as three times the 'measurement standard deviation', vary from sample to sample and is based on the intensity of the X-rays received at the detector; this depends on many factors, including sample composition (the effect of other elements in the same matrix) and analyser/sample geometry. Elements falling below the analysis LoD are not reported, and many elements are below LoD in all analysed samples (for example Se, Te, Au, As and Hg). Other elements however, such as Mg or P, are close to the LoD in some samples and not in others. This provides

https://doi.org/10.1180/mgm.2022.22 Published online by Cambridge University Press

Table 1. List of samples used in this study together with their provenance and reference to any published petrographic descriptions.

Sample number	Lithological grouping	Context	Additional notes*	Petrographic description
FN573	Altar Stone fragment	From a Roman context at Stonehenge	Excavated in 2008 by Darvill and Wainwright. Previously erroneously labelled FN593	Ixer and Bevins (2013)
Spit V/I	Altar Stone fragment	From Context 3 spit V/I from the Stonehenge Layer	Excavated in 2008 by Darvill and Wainwright. Labelled HM13 in Bevins *et al.* (2020)	Ixer and Bevins (2013)
FN196	Altar Stone fragment	From modern overburden at Stonehenge	Excavated in 2008 by Darvill and Wainwright. Labelled SH 08 in Bevins *et al.* (2020)	Ixer and Bevins (2013); Ixer *et al.* (2019)
MS1	Altar Stone fragment	From near stone 1	Excavated by Hawley	Ixer *et al.* (2019)
MS2	Altar Stone fragment	From near stone 1	Excavated by Hawley	Ixer *et al.* (2019)
MS3	Altar Stone fragment	From near stone 1	Excavated by Hawley	Ixer *et al.* (2019)
UORS 6	Old Red Sandstone	Pen-y-Fan Formation	Map ref SO 016112	Hillier *et al.* (2006)
LORS 1	Old Red Sandstone	Brownstones Formation	Map ref SO 043163	Hillier *et al.* (2006)
LORS 34	Old Red Sandstone	Brownstones Formation	Map ref SN 732195	Hillier *et al.* (2006)
WM 3	Old Red Sandstone	Senni Formation	Map ref SO 579848	Hillier *et al.* (2006)
FW 1	Old Red Sandstone	Milford Haven Subgroup	Map ref SR 885993	Hillier *et al.* (2006)
DEV 6	Old Red Sandstone	Moor Cliffs Formation	Map ref ST 312912	Hillier *et al.* (2006)
ORS 6794	Old Red Sandstone	Senni Formation	Map ref SO 16541987	Unpublished

*Map references are UK ordnance survey grid references

Table 2. Operating conditions for the TestAllGeo procedure used to determine the composition of the samples.

pXRF element range	Time (s)	Elements that can be detected using filter*	Elements detected in the majority of analyses in this study
Main Filter	30	Mo, Zr, Sr, U, Rb, Th, Pb, Se, As, Hg, Zn, W, Cu, Ni, Co, Fe, Mn	Zr, Sr, U, Rb, Th, Pb, Zn, Cu, Ni, Fe, Mn
Low Filter	30	Cr, V, Ti, Sc, Ca, K, S	Cr, V, Ti, Ca, K
High Filter	20	Ba, Cs, Te, Sb, Sn, Cd, Ag, Pd, Nb, Bi, Re, Ta, Hf	Ba, Nb
Light Filter	20	Al, P, Si, Ca, K, Cl, S, Mg	Al, P, Si, Mg

*Elements that can be detected with each filter as listed by Niton (Niton XL3t 900 Analyzer with GOLDD Technology Users Guide, Version 6.5)

some useful information from the samples in which these are reported, even if their concentration is too low in other samples. Data for the reported LoD, the lowest recorded concentration, and the number of analyses above the LoD (i.e. cases where an element is reported) are given in Supplemental Table S2.

The pXRF data for materials considered in this paper are presented in Supplemental Table S3. In graphically presenting the pXRF data we have left the concentration as elemental ppm (parts per million m/m) throughout, and only in Table 3 has it been converted to oxide concentrations (as for major elements) to compare with mineralogy. Data are presented either as integer values or rounded to 1 decimal place (when <100 ppm), however it must be remembered that this will considerably over-estimate the precision with which these elements can be determined by pXRF, which is typically in the range of ± 5% based on repeated obsidian analyses (see above, and Supplemental Table S1).

Portable XRF has the advantage of being non-destructive, however there are disadvantages associated with element detection/identification from spectral overlaps, and with calibration and sample homogeneity issues (Hunt and Speakman, 2015). For example, in the majority of analyses the Niton pXRF reported ~2.8 ppm Pd in the Newberry Obsidian and ~1.5 ppm Pd in the Altar Stone and debitage analyses, which are exceptionally high when compared with an average crustal concentration of <1 ppb (GERM, 2021), as well as rare occasions where Au and Hg are reported. In cases such as these, where spectral overlaps or interferences cause unrealistically high concentrations of some elements to occur, or where elements are routinely close to their lower limits of detection, we have excluded these elements from further consideration. Regardless of such drawbacks, pXRF is a rapid and non-destructive method for analysis of natural and man-made materials in archaeological studies (Liritzis and Zacharias, 2011) and is ideal for use where sampling for geochemical analysis by bulk methods is not possible when attempting to confirm correlations based on compositional data between excavated fragments and possible source monolith. Whilst debate ensues about the use of pXRF and its accuracy/precision and calibration (Speakman and Shackley, 2013), it does provide reproducible and acceptably accurate data for comparison and correlation of archaeological materials where like-for-like analyses are conducted in non-destructive provenance studies. Portable XRF has been used

Table 3. Compositions of debitage fragments and Altar Stone recalculated to oxide or compound (marked *) concentrations as wt.%. These have been recalculated using the relative atomic masses from the ppm concentration into weight percentage (wt.%), with all Ca assumed to be present as calcite and all Ba as baryte, which is likely to somewhat overestimate these mineral abundances where some of these elements are associated with other phases (e.g. feldspar or mica).

Oxide or compound (wt.%)	Debitage fragments, average	Altar Stone, average
MgO	1.61	0.84
Al_2O_3	9.38	1.58
SiO_2	63.15	24.83
P_2O_5	0.60	0.32
K_2O	0.98	0.77
$CaCO_3$*	9.35	2.17
TiO_2	0.63	0.41
MnO	0.08	0.07
Fe_2O_3	2.18	1.70
$BaSO_4$*	0.67	0.48
Total	88.64	33.16

https://doi.org/10.1180/mgm.2022.22 Published online by Cambridge University Press

in recent studies of the provenance of the sarsen stones at Stonehenge by Nash *et al.* (2020) who used Bayesian principal component analysis for discrimination purposes. This is better able to accommodate elements that "fluctuate close to or below instrumental detection limits". The sarsens are considerably more silica-rich than the Altar Stone and key discriminant elements in the Altar Stone are at elevated concentrations compared to the sarsen stones.

In situ vs ex situ (wet vs dry) analyses

As reported earlier, we analysed *ex situ* a series of small hand specimens of debitage from the Stonehenge Landscape assumed to be pieces of the Altar Stone recovered from previous archaeological excavations (Bevins *et al.*, 2020) together with six fragments of Old Red Sandstone used for a study of ORS clay mineralogy (Hillier *et al.*, 2006) and one unpublished field sample from the Old Red Sandstone near Llangynidr. These samples were all dry, having spent extended periods of time out of their field setting. The analysed fragments were all >∼1 cm thick, and typically >1.5 cm across, their sizes avoiding any analytical issues associated with signal loss from small samples (Liritzis and Zacharias, 2011; Frahm, 2016). Multiple analyses were performed on different areas of each of these samples (minimum $n = 5$).

The three exposed areas of the Altar Stone at Stonehenge, shown as areas A, B and C on Fig. 2, were analysed by pXRF *in situ* early on the morning of 6th July 2021, during a few clear hours that followed a night of intense rainfall. In total 36 analyses were performed. Standing surface water was mopped from the surface of the Altar Stone with paper towels, however the surface was damp when analysed. We assume the analysed upper surface of the Altar Stone was water saturated, with a porosity (and thus maximum water content) of ∼6–10% based on the characteristics of possible correlative samples (Bevins *et al.*, 2020). Signal attenuation is commonly reported in the analysis of wet materials by pXRF (Kido *et al.*, 2006; Lemiere *et al.*, 2014; Quiniou and Laperche, 2014; Schneider *et al.*, 2016; Goff *et al.*, 2020), this being more extensive the wetter the sample matrix, or when a surface water film is present. Low-energy X-rays (< ∼5 keV; elements lighter than Cr) suffer the greatest attenuation at water contents above 20%. Below this water content low-energy X-ray attenuation is not as severe, and becomes relatively insignificant for high-energy X-rays (Kalnicky and Singhvi, 2001; Ravansari *et al.*, 2020). In thoroughly wet samples (e.g. slurries) attenuation affects both low- and high-energy X-rays. In contrast, for the *ex situ* analysis of dried samples, signal reduction from water is insignificant or absent. We discuss the implications for the pXRF analyses of these *in situ* and *ex situ* materials in the Results section below.

Bevins *et al.* (2020) utilised automated SEM-EDS to quantify the mineralogy of the Altar Stone and its previously assumed source area. As the geochemical response detected using the portable XRF will be controlled by the mineralogy of the sandstones, we have used data presented in Bevins *et al.* (2020) to provide a mineralogical map of a representative example of the Altar Stone debitage (sample FN196), allowing the visualisation of the mineral distribution in the analysed sample. The detailed methodology and results are provided in Bevins *et al.* (2020).

Results

Altar Stone and debitage comparisons

Bivariate plots for a range of elements determined in the debitage fragments and the *in situ* Altar Stone are given in Fig. 3. For many of the heavier elements in these plots it is clear that the range of concentration displayed for the Altar Stone is the same as the range displayed in the debitage fragments (e.g. Sr, Zr, Nb, Th and U), whereas the lighter elements (Mg, Al, Si, K and Ca) are all considerably lower for the Altar Stone. Barium analyses shows a few data that have lower concentrations in the Altar Stone (from Area C) than in the debitage samples, which extend to marginally higher Ba (mostly for MS2), whereas Rb shows slightly lower concentrations in the Altar Stone (25.6 ± 3.1 ppm) compared to the debitage fragments (29.8 ± 3.7 ppm). A Student t-test (performed for each element in Microsoft® Excel, see Table 4) shows that for many of the light elements the average concentrations reported in the Altar Stone are significantly different (at $p<0.05$) from the debitage fragments, though for the heavier elements (Sr and higher atomic numbers) the analyses can be considered to be drawn from the same population. However, the low concentrations of light elements, particularly Si and Al in the Altar Stone, are too low to be correct for a micaceous sandstone. When Mg, Al, Si, P, K, Ti, Mn and Fe are converted to oxides, Ca to $CaCO_3$ and Ba to $BaSO_4$, the average composition from the Altar Stone sums to only 33.1 wt.%, whereas in the debitage fragments these components total 88.6 wt.% (Table 3), a more realistic analytical total.

The average compositions of the debitage fragments and the Altar Stone are compared in Table 4, where the ratio of Altar Stone/debitage average is shown for each element. With increasing element atomic number (Z), this ratio generally increases, being close to unity above $Z \approx 35$, and this is shown in Fig. 4, where this ratio is plotted against element atomic number.

Alhough the high atomic number elements indicate clearly that the debitage fragments are the same composition as the Altar Stone (occupying the same compositional space in Fig. 3 and t-test data in Table 4), the low concentrations of light elements reported by pXRF from the Altar Stone are different. This difference, for most light elements, is interpreted as due to the wet nature of the Altar Stone during analysis, with the presence of water causing significant attenuation of the long wavelength, low energy X-rays emitted from the low-Z elements. In this respect, the results of the *in situ* analysis of the Altar Stone resembles the results from analysis of wet sediment/soil and the attenuation of light-element X-rays explains the low reported concentrations of the light elements (see Table 4). Above $Z = 37$ (Sr and heavier) the Altar Stone/debitage fragments analysis ratio is >0.8, and no statistical difference exists between the analyses of the two samples (from Student t-test results, except for Ba) indicating that they are drawn from the same population, i.e. they are compositionally the same.

The lowest-Z elements in the Altar Stone (Al and Si) are reported at 20–40% of their concentration in the dry debitage samples. The high ratio for Mg (∼0.52) is due to only three Mg results being above the LoD in the Altar Stone, which gives a skewed high average calculated only from those samples where Mg was detected, and ignores the 33 results where it was below detection limits – the expected ratio (if the pXRF LoD for Mg was lower) should be similar to or lower than that for Al. Calcium concentrations ($Z = 20$) appear to be anomalously low in the Altar Stone compared to neighbouring elements (e.g. K and Ti, ratio ≈0.7), with the Altar Stone/debitage fragments ratio ≈0.23. If X-ray attenuation was the cause from the wet analyses, a similar ratio would be expected, hence other processes may be involved here. The automated mineralogy data indicate that the debitage fragments contain between 12.6–16.6 vol.% of

https://doi.org/10.1180/mgm.2022.22 Published online by Cambridge University Press

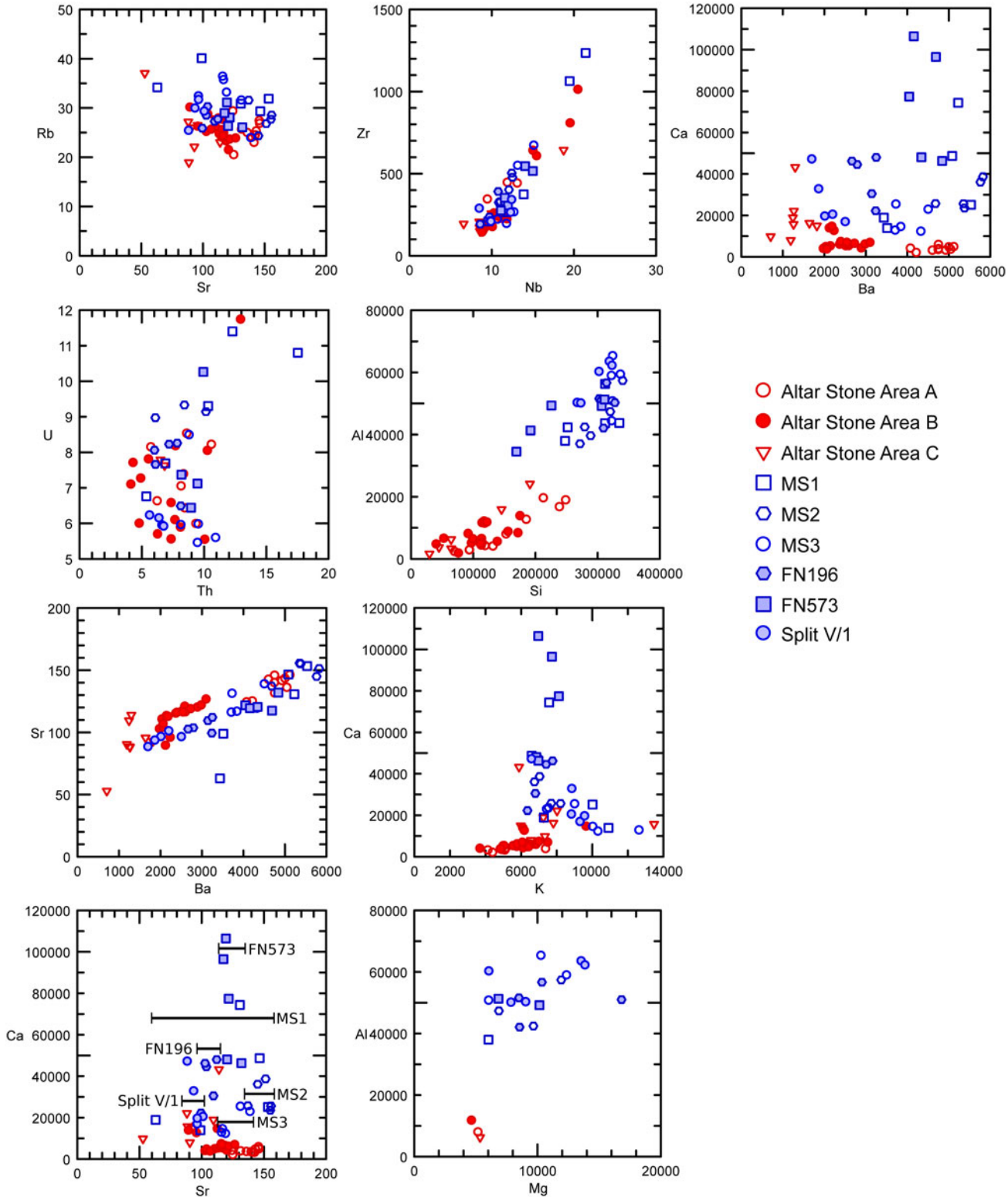

Fig. 3. Elemental biplots of data from pXRF analyses of the Altar Stone ($n = 36$, red symbols) and the debitage fragments ($n = 30$, blue symbols). All concentrations reported as ppm. Note that for some elements several results are not plotted because they fall below the limit of detection (LoD) for that analysis (most notably Mg). The horizontal bars on the Sr vs Ca plot show the range of Sr in individual chips of debitage. Note how the range is more restricted than Ca and that there is no correlation between Sr and Ca in the debitage chips. Sample details presented in Table 1.

calcite cement (data presented in Bevins *et al.*, 2020). The Ca concentration in the debitage fragments suggests ~10% of calcite, illustrated for sample FN196 in Fig. 5 (assuming Ca is not abundantly hosted in other phases) which agrees broadly with the automated mineralogy in the debitage samples, though only calculates as ~2% in the Altar Stone (see Tables 3 and 4). It is

https://doi.org/10.1180/mgm.2022.22 Published online by Cambridge University Press

Table 4: Average composition of the debitage fragment samples and the Altar Stone, arranged in order of increasing atomic number. The ratio Altar Stone/debitage indicates the extent of difference between the two sets of material; note how this ratio gets close to unity as element atomic number (and mass) increases (see also Fig. 4).*

Element (ppm)	Atomic number (Z)	Debitage fragments, average	Debitage fragments, std dev	*n*	Altar Stone, average	Altar Stone, std dev	*n*	Student t-test, p =	Altar Stone/ debitage
Mg	12	9715	3056	18	5064	357	3	0.018	0.521
Al	13	49,679	8335	30	8381	5666	34	<0.001	0.169
Si	14	294,709	41,849	30	115,851	57,129	36	<0.001	0.393
P	15	2628	1249	26	1413	861	31	<0.001	0.538
K	19	8141	1517	30	6342	1705	36	<0.001	0.779
Ca	20	37,389	24,080	30	8680	7772	36	<0.001	0.232
Ti	22	3850	893	30	2520	643	36	<0.001	0.655
V	23	57.2	11.1	28	44.4	8.7	34	<0.001	0.776
Cr	24	65.3	24.0	30	47.5	17.4	36	0.001	0.727
Mn	25	630	118	30	551	333	36	**0.221**	0.875
Fe	26	15,545	2254	30	12,073	1672	36	<0.001	0.777
Ni	28	81.9	18.8	30	59.5	16.1	31	<0.001	0.727
Cu	29	32.5	10.7	30	25.1	5.6	23	0.004	0.774
Zn	30	54.1	12.8	30	69.6	16.1	36	<0.001	1.287
Rb	37	29.8	3.7	30	25.6	3.1	36	<0.001	0.858
Sr	38	119	23	30	115	20	36	**0.417**	0.964
Zr	40	394	240	30	308	198	36	**0.116**	0.782
Nb	41	12.3	2.8	30	11.3	3.1	36	**0.175**	0.919
Mo	42	6.9	3.6	15	6.6	2.4	26	**0.728**	0.953
Ba	56	3914	1206	30	2815	1326	36	0.001	0.719
Pb	82	40.4	21.5	30	32.8	11.0	34	**0.075**	0.812
Th	90	8.5	2.4	29	7.3	2.1	31	**0.055**	0.865
U	92	7.7	1.6	27	7.1	1.3	26	**0.206**	0.931

*Notes: Concentrations are in ppm and are left as either integer or 1 decimal place (when <100 ppm), although this will considerably overestimate the precision with which these elements are determined.
'*n*' is the number of analyses which are above the LoD, and thus where *n* is low (e.g. Mg) the average will be considerably overestimated as the majority of analyses not reported and therefore excluded from the calculation.
The 'Student t-test p =' value is the probability for a two tailed, equal variance t-test performed (in Microsoft® Excel) on the means of each element. Where the p value is given in bold, it is not significant at p<0.05 indicating that the null hypothesis (that analyses are from different populations) can be rejected at the 95% confidence level, and the analyses can be considered to come from the same sample population. Where p<0.05, the samples can be considered to be drawn from different populations at the 95% confidence level.

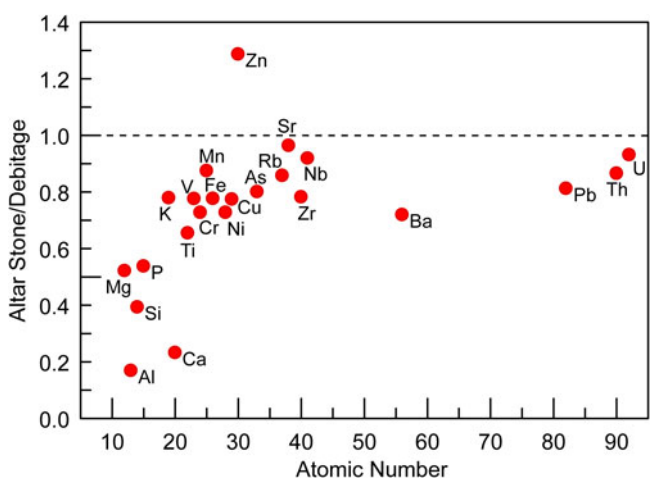

Fig. 4. The ratio of the concentration of an element determined by pXRF in the Altar Stone divided by its concentration in the MS chips, for data where overall there were fewer than 50 analyses in which the particular element was not detected (see Table 4).

possible that leaching of calcite from the exposed surface of the Altar Stone by naturally mildly acidic rainfall (pH ≈ 5.5) has occurred since it was placed at Stonehenge, reducing Ca to very low levels, except in the results from analyses of Area C (see Fig. 3) which may have been somewhat better protected from surface weathering, being under the fallen lintel of the Great Trilithon (stone 156) (see Fig. 2d). The strong correlation of Ba with Sr in both the Altar Stone and debitage fragments (see Fig. 3) suggests that Sr is hosted within baryte (where there is a complete solid solution with celestine), and the lack of a relationship between Ca and Sr in the debitage fragments, which show a wide range of Ca with a limited Sr range (Fig. 3), suggests that Sr is not associated with the calcite cement in this sandstone.

The ratio of average Ba concentrations between the Altar Stone and debitage fragments is also slightly low (~0.72, Table 4, Fig. 4) compared to neighbouring *Z* elements, even though the range of Ba is very similar in both the Altar Stone and the debitage fragments, with the Altar Stone containing slightly lower Ba than the debitage. This suggests two possibilities. Either the differences arise because of the location of the analyses on the Altar Stone (accessible in only a few areas, and only the upper surface), which has a clearly heterogeneous distribution of Ba (Area C has the lowest Ba and Area A the highest), compared to the position on the Altar Stone from where the debitage fragments originated. Alternatively, the exposed surface of the Altar Stone may have had some baryte cement leached from it due to several thousand years of exposure to mildly acidic rainfall. The automated mineralogy results show baryte to be depleted/removed from the margins of some debitage fragments (e.g. in FN196; see Fig. 5). This is consistent with reduced baryte solubility in the alkaline (pH ~8), carbonate-bearing chalk soil environment of Salisbury Plain compared to the exposed Altar Stone surface (Carbonell *et al.*, 1999; Macphail and Crowther, 2008). As suggested for calcite, baryte may have been leached from the surface of the Altar Stone over the last few thousand years. In contrast to baryte, however, there is no observed reduction of calcite from the margins of the debitage fragments (see Fig. 5) suggesting that a different process is responsible for the leaching of the baryte. The

https://doi.org/10.1180/mgm.2022.22 Published online by Cambridge University Press

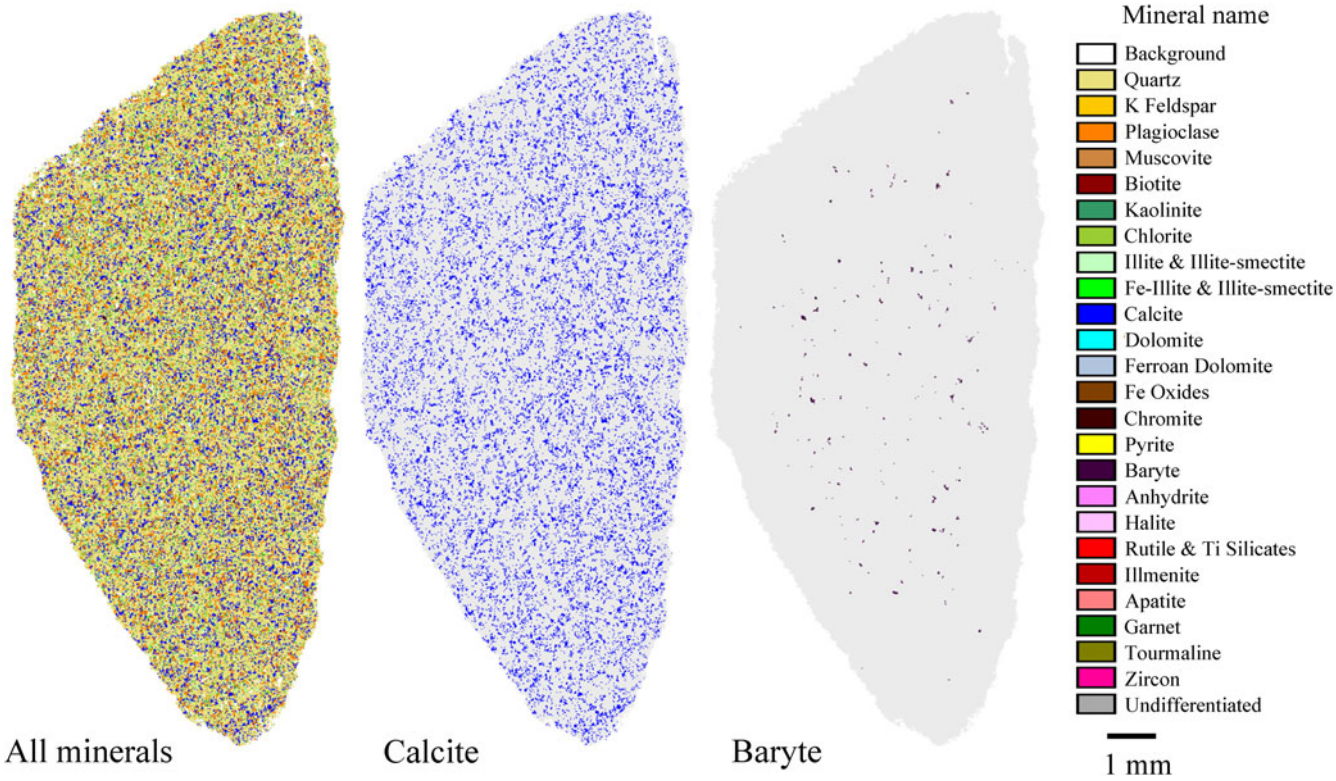

Fig. 5. Automated SEM-EDS mineral maps highlighting the distribution of calcite and baryte in debitage sample FN 196 as an example. Data and methodology are presented in Bevins *et al.* (2020). Images show: (a) the distribution of all minerals; (b) the distribution of calcite; and (c) the distribution of baryte.

debitage samples were buried in moderately carbonate-rich soils and thus protected from the direct effects of acidic rainfall. In particular, the solubility of the baryte might have been increased by bacterial activity (Phillips *et al.*, 2001; Ouyang *et al.*, 2017). Analyses of a profile through to the deeper, buried part of the Altar Stone (see Fig. 2c), when next excavated, may help to confirm this hypothesis.

In summary, the dry *ex situ* pXRF analyses of the various debitage fragments provide consistent data for a range of light and heavy elements, whereas the wet, *in situ* analyses of the Altar Stone are affected adversely by attenuation of low energy X-rays, making only the data for high-*Z* elements reliable. Data from both materials for the high-*Z* elements (e.g. Sr, Zr, Nb, U and Th) clearly show the debitage fragments are compositionally indistinguishable from the *in situ* Altar Stone. Both debitage fragments and the Altar Stone have suffered leaching of baryte over the millennia, and some calcite dissolution also appears to have occurred from the *in situ* Altar Stone, however the relatively lower solubility of baryte has meant only a moderate change in the Ba concentrations over time.

Altar Stone and ORS comparisons

Having shown above that a range of sandstone debitage fragments are compatible with a derivation from the Altar Stone, we now consider these results as Altar Stone (*sensu lato*) for comparison with a small selection of samples of potential source rocks from the Old Red Sandstone of Wales and the Welsh Borderland. We focus on this area in view of the previous suggestions that the Altar Stone was derived from lithologies assigned to the Old Red Sandstone (see Thomas, 1923). The objective of this is to determine whether rapid pXRF analysis of sandstone field samples might provide a viable means of testing for a potential source for the Altar Stone, acknowledging that this is a very small sample set for a geological division that covers a wide geographic area. The samples were a sub-set of those analysed for their clay mineralogy by X-ray diffraction by Hillier *et al.* (2006) as well as a single unpublished field sample and were drawn from a broad geographical range (Fig. 1).

Five bivariate plots of a range of high-*Z* elements for the Altar Stone (*sensu lato*) results are shown in Fig. 6 together with four bivariate plots that compare low-*Z* elements or ratios from only the debitage fragments because, as noted above, these light elements are affected by the attenuation of the X-ray emission in the wet, *in situ* Altar Stone analyses. Table 5 shows the average compositions of the Altar Stone (*sensu lato*, excluding the low-*Z* *in situ* Altar Stone analyses) compared to the ORS results, and includes the p value for a Student t-test on these data. It is clear from Fig. 6 and Table 5 that significant differences exist between the composition of the various ORS samples analysed and the Altar Stone, the latter having Ba and Sr that far exceed almost all of the ORS samples, and trace-element ratios, such as Rb/Ba, Ba/Sr, Sr/Rb that are all considerably different. Zirconium shows much higher contents in the Altar Stone samples (and must reflect higher detrital zircon contents); however, Nb, Th and U (limited numbers of analyses) all have broadly similar concentrations. For the major and minor elements, K is higher in all the ORS samples, and Al/K ratios are significantly different, which will probably reflect different mineralogical contents, notably feldspar, mica and clay. Titanium has a similar range in the Altar Stone and ORS samples, suggesting similar Fe–Ti oxide contents, however P is higher in the Altar Stone, suggestive of higher detrital

https://doi.org/10.1180/mgm.2022.22 Published online by Cambridge University Press

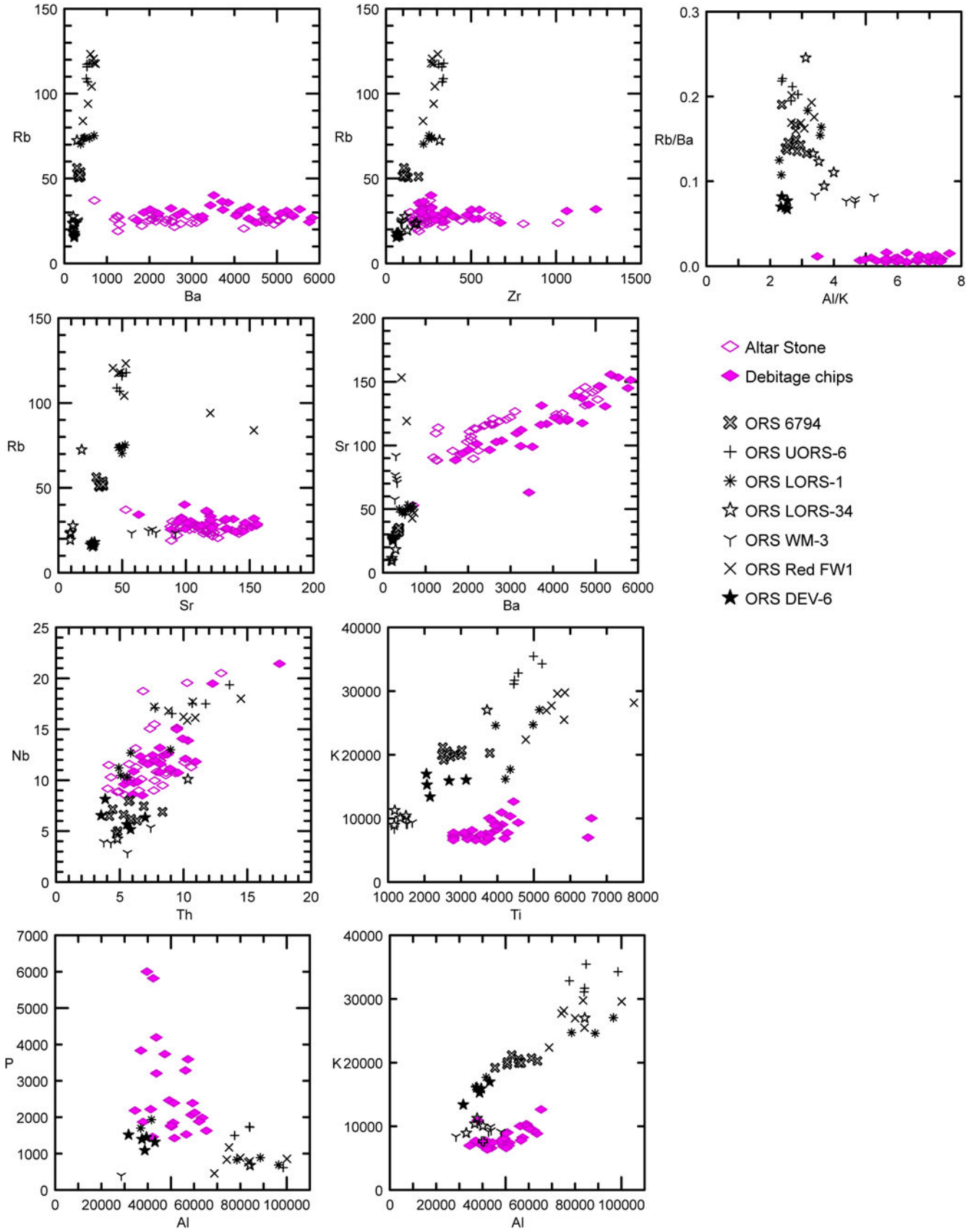

Fig. 6. Comparison of the composition of the Altar Stone (*sensu lato*) with a range of Old Red Sandstone samples from Wales and the Welsh Borderland. For the major elements, which are affected by attenuation of the X-ray emission by water in the *in situ* analysis of the Altar Stone, only the results from analyses of debitage chips are included. All concentrations in ppm.

https://doi.org/10.1180/mgm.2022.22 Published online by Cambridge University Press

Table 5: Average composition of the Altar Stone (*sensu lato*) and the ORS samples analysed, with the low-*Z* elements determined in the Altar Stone excluded from the calculation of the average.*

Element (ppm)	Altar Stone (*s.l.*), average	Altar Stone, std dev	ORS samples, average	ORS samples, std dev	Student t-test, p=
Mg	9715	3056	11,336	4465	**0.178**
Al	49,679	8335	59,872	21,110	0.015
Si	294,709	41,849	298,516	46,847	**0.723**
P	2628	1249	1079	446	<0.001
K	8141	1517	20,439	7819	<0.001
Ca	37,389	24,080	13,483	23,349	<0.001
Ti	3850	893	3418	1639	**0.194**
V	57.2	11.1	73.6	30.5	0.009
Cr	65.3	24.0	65.3	37.6	**0.998**
Mn	630	118	758	936	**0.462**
Fe	15,545	2254	20,569	11,830	0.025
Ni	81.9	18.8	60.1	21.2	<0.001
Cu	32.5	10.7	64.3	106.5	**0.109**
Zn	54.1	16.5	47.9	33.2	0.003
Rb	27.5	4.0	61.6	36.7	<0.001
Sr	118	21	45.3	27.6	<0.001
Zr	353	221	183	96	<0.001
Nb	11.8	3.0	9.9	5.3	0.024
Mo	6.7	2.8	4.3		
Ba	3368	1378	405	159	<0.001
Pb	36.6	17.0	18.3	10.5	<0.001
Th	8.0	2.3	7.1	2.8	**0.155**
U	7.4	1.5	9.3	1.7	0.001

*Notes: Concentrations are in ppm. The 'Student t-test p =' value is the probability for a two tailed, equal variance t-test performed (in Microsoft® Excel) on the means of each element. Where the p value is given in bold, it is not significant at p<0.05 indicating that the null hypothesis (that analyses are from different populations) can be rejected, and the analyses can be considered to come from the same sample population: note that the majority of elements are statistically significantly different.

phosphate (apatite). From the differences in composition, it can be concluded that the Altar Stone source is not represented by the, albeit very limited, ORS samples analysed as comparators here, and differs markedly in K/Al, Ba/Rb, Zr, Sr and P.

Discussion and implications for future investigations

The intent of this study was to determine if the data from pXRF analysis of derived debitage fragments could be used to match them to a source monolith, using the Stonehenge Altar Stone as a case study. If successful it would mean that the presumed debitage fragments could be used as a proxy for the *in situ* Altar Stone, allowing for analysis of the fragments whilst preserving the integrity of the monument itself. These analytical investigations would then provide data relevant to determining a provenance for the Altar Stone.

In order to test whether this is a valid approach we sought (and obtained) permission to analyse the Altar Stone using the non-destructive pXRF technique. One significant problem we encountered related to the damp conditions experienced during *in situ* analysis of the Altar Stone. The effect of analysing a damp surface is attenuation of the X-ray emission from low-*Z* elements; we found that this affects elements with atomic numbers below $Z = 37$. However, for elements with $Z > 37$ there is a good correlation between the Altar Stone element contents and those in the *ex situ* fragments and hence we consider the results from the Altar Stone analyses for the heavier elements to be reliable. On this basis we believe that the data obtained in this study support the previous correlation between the Altar Stone and the debitage fragments hitherto presumed to have been derived from it based on lithological similarity alone. As a consequence, we are able to use the data obtained previously from the presumed debitage fragments, as reported in Ixer *et al.* (2020) and Bevins *et al.* (2020), in our search for the source of the Altar Stone. A notable feature of the Altar Stone, based on automated SEM-EDS analysis of the debitage fragments, is the relatively high modal % of baryte, which is confirmed by the Ba contents identified by pXRF in this study. This characteristic is likely to be of considerable significance and utility in provenancing the Altar Stone.

This study has shown that regardless of the well-publicised shortcomings of the pXRF technique, including the effects of analysing wet material surfaces, the technique does offer scope for the rapid matching of debitage fragments to source monolith. This provides a method for the non-destructive analysis of lithic components of ancient monuments whilst preserving the integrity of the monument itself.

The next stage in our investigation of the potential source of the Stonehenge Altar Stone is to collate and interpret the mineralogical and geochemical data obtained to date on the derived fragments in order to compile a detailed picture of its possible source rock. In particular we aim to understand the relationship between the calcite and the baryte as this will provide insight into the rock's diagenetic history.

As noted above, Thomas (1923) proposed a potential source for the Altar Stone in the Old Red Sandstone sequences of South Wales. However, as Bevins and Ixer (2018) noted, Thomas was convinced that all of the bluestones (except the Altar Stone) were derived from a very limited geographical area in the Mynydd Preseli, in north Pembrokeshire. We consider it probable that Thomas considered the nearest source of the ORS to the Mynydd Preseli as the most likely source for the Altar Stone. Critically, however, there is no direct geological evidence to support an ORS age for the Altar Stone. Interestingly, one of the earliest references to a possible Devonian age for the Altar Stone was in a letter from Professor John Phillips of Oxford University to archaeologist Dr John Thurnam of Devizes, dated 22nd December 1858, in which he suggested that it may be derived from the "gray *Devonian* or gray Cambrian rocks.." (see Long, 1876). Phillips was appointed to the Chair of Geology at King's College London in 1834 and in 1839 published his 'Report on the Geology of Cornwall, Devon and west Somerset'. His 'gray Devonian' might well be reference to the marine Devonian sequences of southwest England rather than the continental (predominantly red) Old Red Sandstone sequences of south Wales and the Welsh Borderland. Perhaps of significance is the fact that by the time this possible source for the Altar Stone is mentioned by Maskelyne (1878) he omits the descriptor 'gray', referring only to the "..Devonian or gray Cambrian rocks..", and then proceeding to note that his assistant at the British Museum, Mr Thomas Davies, drew to Maskelyne's attention the occurrence of "just such a rock at the top of the old red sandstone (sic) cropping out no further off than Frome". Perhaps this is where the link between the Altar Stone and the Old Red Sandstone derives from. This leads us to keep an open mind over the potential source of the Altar Stone, especially as we are not aware of any reports of baryte-bearing sandstones in the Old Red Sandstone sequences of Wales or the Welsh Borderland.

Conclusions

We tested the potential link between debitage fragments from excavations at Stonehenge identified visually as being derived

https://doi.org/10.1180/mgm.2022.22 Published online by Cambridge University Press

from the Stonehenge Altar Stone by pXRF to ascertain if the visual link was valid. The Altar Stone was analysed *in situ* on a wet morning following a night of rain, contrasting with the *ex situ*, dry setting for the debitage fragments. Accordingly, the surface of the Altar Stone at the time of analysis was wet. This caused attenuation of the signal for light elements (below $Z = 37$). However, strong correlations for elements above $Z = 37$ leads us to conclude that the fragments were indeed derived from the Altar Stone. This shows that even though there are widely publicised concerns over the pXRF technique, in this case it did provide a credible geochemical comparison between the derived fragments and source monolith and highlights the value of the technique in this particular archaeological context. In addition, being a non-destructive technique, it does not compromise the integrity of the ancient monument.

Having matched the derived fragments to the Altar Stone we are now in a position to interpret with confidence the data obtained to date on the derived fragments in the search for the source of the Altar Stone. The pXRF results showed the Altar Stone to have high Ba contents which is in agreement with the high modal % baryte identified previously using automated SEM-EDS analysis. This rather unusual mineralogy will be a key element in our search for the origin of the Altar Stone.

Acknowledgements. The lead author dedicates this contribution to his close friend Professor Peter Williams who he had the extreme pleasure of working with while Pete was in the Department of Chemistry at Cardiff University in the 1980s. It was an extremely stimulating experience and led, amongst other achievements, to the identification of two new minerals, namuwite (named after the **Na**tional **Mu**seum of **W**ales) and the less provocatively named lanthanite-(Ce). Thank you so much Pete. Professor Tim Darvill (University of Bournemouth) and David Dawson (Wiltshire Museum) are thanked for access to the excavated debitage samples used in this study. Helen Woodhouse (Historic England) and Heather Sebire and Susan Greaney (English Heritage) are thanked for arranging permission and facilitating access to the Altar Stone and for the agreement to analyse it. Jackie Chadwick is thanked for expertly producing Fig. 1. The lead author gratefully acknowledges financial support for this work through a Leverhulme Trust Emeritus Fellowship.

Supplementary material. To view supplementary material for this article, please visit https://doi.org/10.1180/mgm.2022.22

References

Bevins R.E. and Ixer R.A. (2018) Retracing the footsteps of H.H. Thomas: a review of his Stonehenge bluestone provenancing study. *Antiquity*, **363**, 788–802.

Bevins R.E., Ixer R. A., Webb P.C. and Watson J.S. (2012) Provenancing the rhyolitic and dacitic components of the Stonehenge landscape bluestone lithology: new petrographical and geochemical evidence. *Journal of Archaeological Science*, **39**, 1005–1019.

Bevins R.E., Ixer R.A. and Pearce N.J.G. (2014) Carn Goedog is the likely major source of Stonehenge doleritic bluestones: evidence based on compatible element geochemistry and Principal Component Analysis. *Journal of Archaeological Science,* **42**, 179–193.

Bevins R.E., Pirrie D., Ixer R.A., O'Brien H., Parker Pearson M., Power M.R. and Shail R.K. (2020) Constraining the provenance of the Stonehenge 'Altar Stone': Evidence from automated mineralogy and U-Pb zircon age dating. *Journal of Archaeological Science*, **120**, 105188.

Bevins R.E., Pearce N.J.G. and Ixer R.A. (2021) Revisiting the provenance of the Stonehenge bluestones: refining the provenance of the Group 2 non-spotted dolerites using rare earth element geochemistry. *Journal of Archaeological Science: Reports,* **38**, 103083.

Carbonell A.A., Pulido R., De Laune R.D. and Patrick W.H. (1999) Soluble barium in barite and phosphogypsum amended Mississippi River alluvial sediment. *Journal of Environmental Quality*, **28**, 316–321.

Darvill T. and Wainwright G. (2009) Stonehenge excavations 2008. *Antiquaries Journal*, **89**, 1–19.

Darvill T., Marshall P., Parker Pearson M. and Wainwright G. (2012) Stonehenge remodelled. *Antiquity*, **86**, 1021–1040.

Frahm E. (2016) Can I get chips with that? Sourcing small obsidian artifacts down to microdebitage scales with portable XRF. *Journal of Archaeological Science: Reports*, **9**, 448–467.

GERM (2021) *Geochemical Earth Reference Model (GERM) Reservoir Database*, https://earthref.org/GERMRD/.

Goff K., Schaetzl R.J., Chakraborty S., Weindorf D.C., Kasmerchak C. and Bettis III E.A. (2020) Impact of sample preparation methods for characterizing the geochemistry of soils and sediments by portable X-ray fluorescence. *Soil Science Society of America Journal*, **84**, 131–143.

Higgins M.W. (1973) Petrology of Newberry volcano, central Oregon. *Geological Society of America Bulletin*, **84**, 455–488.

Hillier S., Wilson M. and Merriman R. (2006) Clay mineralogy of the Old Red Sandstone and Devonian sedimentary rocks of Wales, Scotland and England. *Clay Minerals*, **41**, 433–471.

Hunt A.M. and Speakman R.J. (2015) Portable XRF analysis of archaeological sediments and ceramics. *Journal of Archaeological Science*, **53**, 626–638.

Ixer R.A. and Bevins R.E. (2013) Chips off the old block: The Stonehenge debitage dilemma. *Archaeology in Wales*, **52**, 11–22.

Ixer R.A. and Turner P. (2006) A detailed re-examination of the petrography of the Altar Stone and other non-sarsen sandstones from Stonehenge as a guide to their provenance. *Wiltshire Archaeology and Natural History Magazine*, **99**, 1–9.

Ixer R.A., Turner P., Molyneux S. and Bevins R.E. (2017) The petrography, geological age and distribution of the Lower Palaeozoic Sandstone debitage from the Stonehenge Landscape. *Wiltshire Archaeology and Natural History Magazine*, **110**, 1–16.

Ixer R.A., Bevins R.E., Turner P., Power M. and Pirrie D. (2019) Alternative Altar Stones? Carbonate-cemented micaceous sandstones from the Stonehenge Landscape. *Wiltshire Archaeology and Natural History Magazine,* **112**, 1–13.

Ixer R.A., Bevins R.E., Pirrie D., Turner P. and Power M. (2020) 'No provenance is better than wrong provenance': Milford Haven and the Stonehenge sandstones. *Wiltshire Archaeology and Natural History Magazine,* **113**, 1–15.

Judd J.W. (1902) Note on the nature of and origin of the rock-fragments found in the excavations made at Stonehenge by Mr Gowland in 1901. In Gowland, W. Recent excavations at Stonehenge. *Archaeologia*, **58**, 106–118.

Kalnicky D.J. and Singhvi R. (2001) Field portable XRF analysis of environmental samples. *Journal of Hazardous Materials*, **83**, 93–122.

Kido Y., Koshikawa T. and Tada R. (2006) Rapid and quantitative major element analysis method for wet fine-grained sediments using an XRF microscanner. *Marine Geology*, **229**, 209–225.

Laidley R.A. and McKay D.S. (1971) Geochemical examination of obsidians from Newberry Caldera, Oregon. *Contributions to Mineralogy and Petrology*, **30**, 336–342.

Lemiere B., Laperche V., Haouche L. and Auger P. (2014) Portable XRF and wet materials: application to dredged contaminated sediments from waterways. *Geochemistry: Exploration, Environment, Analysis*, **14**, 257–264.

Linneman S.R. (1990) *The Petrologic Evolution of the Holocene Magmatic System of Newberry Volcano, Central Oregon*. PhD thesis, University of Wyoming, Laramie, USA, 312pp.

Liritzis I. and Zacharias N. (2011) Portable XRF of archaeological artifacts: current research, potentials and limitations. Pp. 109–142 in: *X-ray fluorescence spectrometry (XRF) in Geoarchaeology* (M. Shackley, editor). Springer, New York.

Long W. (1876) Stonehenge and its barrows. *Wiltshire Archaeology and Natural History Magazine*, **16**, 1–244.

Macphail R.I. and Crowther J. (2008) *Archaeology on the A303 Stonehenge Improvement: Appendix 1: Soil*. The Highways Agency, Wessex Archaeology, UK.

Maskelyne N.S. (1878) Stonehenge; the petrology of its stones. *Wiltshire Archaeology and Natural History Magazine,* **17**, 147–160.

Nash D.J., Ciborowski T.J.R., Ullyot J.S., Parker pearson M., Darvill T., Greaney S., Maniatis G. and Whitaker K.A. (2020) Origins of the sarsen megaliths at Stonehenge. *Science Advances*, **6**, eabc0133.

https://doi.org/10.1180/mgm.2022.22 Published online by Cambridge University Press

Ouyang B., Akob D.M., Dunlap D. and Renock D. (2017) Microbially mediated barite dissolution in anoxic brines. *Applied Geochemistry*, **76**, 51–59.

Parker Pearson M., Pollard J., Richards J., Tilley C. and Welham K. (2020) *Stonehenge for the Ancestors. Part 1: Landscape and Monuments.* Sidestone, Leiden, Netherlands.

Phillips E.J.P., Landa E.R., Kraemer T. and Zielinski R. (2001) Sulfate-reducing bacteria release barium and radium from naturally occurring radioactive material in oilfield barite. *Geomicrobiology Journal*, **18**, 167–182.

Quiniou T. and Laperche V. (2014) An assessment of field-portable X-ray fluorescence analysis for nickel and iron in laterite ore (New Caledonia). *Geochemistry: Exploration, Environment, Analysis*, **14**, 245–255.

Ravansari R., Wilson S.C. and Tighe M. (2020) Portable X-ray fluorescence for environmental assessment of soils: Not just a point and shoot method. *Environment International*, **134**, 105250.

Schneider A.R., Cancès B., Breton C., Ponthieu M., Morvan X., Conreux A. and Marin B. (2016) Comparison of field portable XRF and aqua regia/ICPAES soil analysis and evaluation of soil moisture influence on FPXRF results. *Journal of Soils and Sediments*, **16**, 438–448.

Speakman R.J. and Shackley M.S. (2013) Silo science and portable XRF in archaeology: a response to Frahm. *Journal of Archaeological Science*, **40**, 1435–1443.

Teall J.J.H. (1894) Notes on sections of Stonehenge rocks belonging to Mr W. Cunnington. *Wiltshire Archaeology and Natural History Magazine,* **27**, 66–68.

Thomas H.H. (1923) The source of the stones of Stonehenge. *The Antiquaries Journal*, **3**, 239–60.

Thorpe R.S., Williams-Thorpe O., Jenkins D.G. and Watson J.S. with contributions by R.A. Ixer and R.G. Thomas (1991). The Geological Sources and Transport of the Bluestones of Stonehenge, Wiltshire, UK. *Proceedings of the Prehistoric Society*, **57**, 103–157.

https://doi.org/10.1180/mgm.2022.22 Published online by Cambridge University Press